

# Storage of Quantum Coherences as Phase Labeled Local Polarization in Solid State NMR

María Belén Franzoni,\* Rodolfo H. Acosta,† Horacio M. Pastawski,‡ and Patricia R. Levstein§  
*Facultad de Matemática, Astronomía y Física and Instituto de Física Enrique Gaviola (CONICET),  
 Universidad Nacional de Córdoba, 5000 Córdoba, Argentina*

Nuclear spins are promising candidates for quantum information processing because their good isolation from the environment precludes the rapid loss of quantum coherence. Many strategies have been developed to further extend their decoherence times. Some of them make use of decoupling techniques based on the Carr–Purcell and Carr–Purcell–Meiboom–Gill pulse sequences. In many cases, when applied to inhomogeneous samples, they yield a magnetization decay much slower than the Hahn echo. However, we have proved that these decays cannot be associated with longer decoherence times as coherences remain frozen. They result from coherences recovered after their storage as local polarization and thus they can be used as memories. We show here how this freezing of the coherent state, which can subsequently be recovered after times longer than the natural decoherence time of the system, can be generated in a controlled way with the use of field gradients. A similar behaviour of homogeneous samples in inhomogeneous fields are demonstrated. It is emphasized that the effects of inhomogeneities in solid state NMR, independently of their origin, should not be disregarded as they play a crucial role in multipulse sequences.

PACS numbers: 03.65.Yz, 76.20.+q, 76.60.Lz, 82.56.Jn

## I. INTRODUCTION

The initial proposals for quantum information processing<sup>1</sup> triggered a worldwide effort to develop simple specific realizations.<sup>2,3</sup> In the last decade, much effort has been devoted to understand and control decoherence<sup>4</sup> as it has become the main drawback for quantum information processing<sup>5–9</sup>.

Within solid state Nuclear Magnetic Resonance the interest focuses in those systems which have been proposed as possible candidates for quantum registers<sup>10–13</sup>, quantum channels<sup>14–16</sup>, simulators of quantum dynamics<sup>17,18</sup> or probes for specific quantum gates<sup>6</sup>.

More, recently, a number of interesting works seek to control the nuclear and electron spin entanglement in systems where the nuclear spins can be used as quantum spin memories such as N@C<sub>60</sub><sup>19</sup>, or <sup>31</sup>P<sup>20</sup> or nitrogen vacancies (NV centers) in diamond<sup>21–23</sup>. Some of the strategies implemented with NMR and EPR, such as decoupling techniques<sup>24–28</sup>, have a wide interest as they can be adapted to many other two level systems like trapped ions, quantum dots<sup>29</sup> or Josephson junctions<sup>30–33</sup>. The renovated interest in pulse sequences that help to fight decoherence has revived the old sequences such as the Hahn Echo<sup>34</sup>, the Carr–Purcell (CP)<sup>35</sup> and the Carr–Purcell–Meiboom–Gill (CPMG)<sup>36</sup> and it has stimulated the development of new ones<sup>37,38</sup>. The simplest dynamical decoupling (DD) sequences consist on the application of  $\pi$  pulses on the system to revert the decay due to the system–environment interactions. Many works have been done in order to compare the performance of the CPMG-like sequences and de Uhrig (UDD) sequences<sup>38</sup> when the system is coupled to a spin bath<sup>27,39</sup>. Yang, Wang and Liu have made a comprehensive theoretical and experimental description of the DD techniques and its variations<sup>40</sup>.

In this work we will make a critical review of recent attempts to extend the decoherence time of spins in solid state NMR or EPR. We show that the role of line inhomogeneity should not be underestimated to observe coherences reliably.

We summarize our own findings on anomalous long lived echo signals<sup>12,41–44</sup>. In particular we emphasize the use of a simple stimulated echo sequence to discern if one is in the presence of true long decoherence times or if the coherences are being saved as polarization and then recovered. This understanding allows us to develop a new strategy for their use that is reported here. It makes use of magnetic field gradients that enable to store part of the phase information as polarization. We demonstrate that inhomogeneous samples in presence of homogeneous fields behave in the same manner than homogeneous samples in presence of inhomogeneous fields.

Additionally, the correct phase cycle to use in multipulse sequences in order to measure the true  $T_2$  in inhomogeneous samples is shown. This sequence, whose result has been empirically known<sup>45–47</sup>, should be taken as a standard to obtain a clean  $T_2$  measurement. Here, we explain how the stimulated echoes are canceled out eliminating their main effects: the long tails.

## II. BASIC NMR CONCEPTS

A typical NMR experiment requires at least two magnetic fields: a static field  $B_0$ , conventionally in the  $z$  direction, and a perpendicular radiofrequency (RF) field  $B_1$  applied to induce transitions. The time  $t_p$  during which the RF is on is defined as the pulse time and the tilting angle is  $\theta_p = \gamma B_1 t_p$ , where  $\gamma$  is the gyromagnetic factor. The eigenstates of angular momentum for a spin  $1/2$  along the static field direction are  $|\uparrow\rangle$  and  $|\downarrow\rangle$ . Once

the thermal equilibrium is reached the population of state  $|\uparrow\rangle$  is larger than that of  $|\downarrow\rangle$  indicating a net polarization of spins along the static field direction. This thermal polarization will determine the maximum magnetization that can be created in the system. Any other situation in which the macroscopic magnetization points in an arbitrary direction will eventually have a z-magnetization which reflects a non equilibrium polarization. A particular but very relevant case is the application of a  $\frac{\pi}{2}$  or saturation pulse after which the magnetization lies in the xy plane. The population of the states is equilibrated and converted in a superposition state (a coherence) where the eigenstates  $|\uparrow\rangle$  and  $|\downarrow\rangle$  have the same probability and a well defined phase relation. The essential difference between polarization and coherences is that, in a very good approximation, polarization does not evolve under interaction with the static field while the transverse magnetization (or coherence) does.

Thus, after a  $\frac{\pi}{2}$  pulse is applied, transverse magnetizations associated with different volume elements (called isochromats) evolve under different Hamiltonians due to small inherent inhomogeneities and spin-spin interactions. This evolution causes a dephasing among the spins in the sample and a free induction decay (FID) with characteristic time  $T_2^*$  is observed. The dephasing caused by inhomogeneities is reversible, so that refocusing is possible by applying appropriate pulse sequences such as the Hahn echo<sup>34</sup> [HE:  $(\frac{\pi}{2} - \tau - \pi - \tau - \text{echo})$ ]. During the evolution time  $\tau$  a dephasing occurs and then a  $\pi$  pulse is applied. The net effect of this pulse is to change the sign of all the Hamiltonians linear in spin operators, thus reversing the evolution of the isochromats which refocus after the same time  $\tau$ . As a result a magnetization echo is observed, i.e. the coherent state created after the initial  $\frac{\pi}{2}$  pulse is partially recovered after a time  $2\tau$ . The amplitude of the echo obtained after a single refocusing pulse is attenuated by homonuclear interactions represented by non linear terms in the system Hamiltonian. In solids the most important contribution will be the spin-spin dipolar interaction. If the separation time  $\tau$  between the pulses is increased a decay in the magnetization is observed with a characteristic time  $T_2$ . This quantity is known as the spin-spin decay time, transverse relaxation or decoherence time. Actually,  $T_2$  represents the decoherence of a single spin caused by its interactions with other spins after canceling out the interactions linear in spins. Indeed, the spin-spin interaction can also be reversed by suitable sequences. They extend the decoherence time to a new timescale  $T_3 > T_2$  characterizing the ability to control the many-body dynamics<sup>17,48-50</sup>. Since, these sequences revert many-body interactions in recent years the quantum information community refers to them as Loschmidt Echoes<sup>17,51-54</sup>. In any case, the decoherence time  $T_2$  is the characteristic time that should be very well known before any attempt of quantum processing. It imposes a first natural limit to quantum control, beyond which more sophisticated experiments that restore phase information (e.g. decoupling and Loschmidt Echo time re-

versal strategies) are needed<sup>17,48-50</sup>. Since 1950, several sequences have been developed in NMR to obtain the  $T_2$  decay time. As the Hahn echo experiment is very time consuming, multipulse sequences that enable the acquisition of the full decay with a single train of pulses such as the Carr-Purcell<sup>35</sup> CP :  $(\frac{\pi}{2})_x - [\tau - \pi_x - \tau - \text{echo}]_n$  and the Carr-Purcell-Meiboom-Gill<sup>36</sup> CPMG :  $(\frac{\pi}{2})_x - [\tau - (\pi)_y - \tau - \text{echo}]_n$  are the most commonly used.

### III. LONG LIVED SIGNALS

The interest in nuclear spins for QIP, in particular silicon<sup>55</sup>, focused on systems where nuclei couple to electron spins which are good candidates for hybrid technologies. This motivated many NMR works where typical experiments to measure  $T_2$  were reported<sup>12,13,56</sup>. In these works after applying the CPMG like sequences it was found that it is possible to detect the spin-1/2 NMR signal of  $^{29}\text{Si}$  up to times much longer (more than two orders of magnitude) than the characteristic decay time observed with the Hahn echo sequence ( $\approx 5.6$  ms). This striking and promising finding came as a surprise and triggered the realization of many experiments to understand its origin. From the beginning it was verified that there is no dependence on the amount of donors or acceptors in the  $^{29}\text{Si}$  polycrystalline sample even when these could change the linewidths and spin-lattice relaxation time by one order of magnitude. Experiments were repeated on  $^{29}\text{Si}$  single crystals and Pyrex, as well as  $^{13}\text{C}$  in  $\text{C}_{60}$  yielding the same behavior.

Since the measurements were performed in natural abundance  $^{29}\text{Si}$  (4.67%) and  $^{13}\text{C}$  (1.1%), it was clear that the spins are diluted yielding weakly coupled networks. Notice that the spin dipolar interactions decay with the cube of the distance and that the gyromagnetic factors of  $^{29}\text{Si}$  and  $^{13}\text{C}$  are approximately one fifth and one fourth of the  $^1\text{H}$  rendering  $^{29}\text{Si}$ - $^{29}\text{Si}$  and  $^{13}\text{C}$ - $^{13}\text{C}$  couplings which are 1/25 and 1/16 of the  $^1\text{H}$ - $^1\text{H}$  respectively. This suggests that the disorder of the chemical shift energies (or site energies) in such weakly coupled networks could play a relevant role in the observed phenomena, which have not been observed in the popular proton samples (ie. in solid state NMR of  $^1\text{H}$  the usual observation is that the results from a Hahn echo coincides with those of the CP or CPMG sequences). With this in mind we started a series of experiments and calculations in a natural abundance polycrystalline sample of  $\text{C}_{60}$ . The first experiment was a traditional Hahn echo measurement as a function of the time  $\tau$  which yielded  $T_2^{HE} \simeq 15$  ms. It should be noted that the decay of the FID revealed a  $T_2^* \simeq 2$  ms, indicating a high degree of inhomogeneities or reversible single spin interactions. Then, we used a series of different trains, derived from the CP and CPMG sequences. These sequences were named respecting their origin (CP or CPMG for  $\pi$  pulses with  $0^\circ$  or  $90^\circ$  phase shifts with respect to the first  $\frac{\pi}{2}$  pulse, respectively) and considering

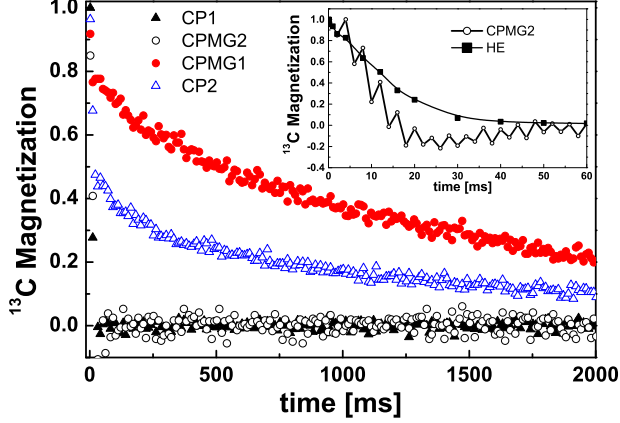


FIG. 1: Comparison of the  $^{13}\text{C}$  magnetizations acquired with different  $T_2$  sequences ( $\tau = 1$  ms). The insert shows the decay observed with the Hahn echo and the short time regime of the CPMG2 sequence.

the number of phases (1 or 2) for the  $\pi$  pulses in each cycle as follows:

$$\text{CP1} : \left(\frac{\pi}{2}\right)_x - [\tau - (\pi)_x - \tau - \text{echo}]_n, \quad (1a)$$

$$\text{CP2} : \left(\frac{\pi}{2}\right)_x - \left[ \begin{array}{l} \tau - (\pi)_x - \tau - \text{echo} \\ \tau - (\pi)_{-x} - \tau - \text{echo} \end{array} \right]_n, \quad (1b)$$

$$\text{CPMG1} : \left(\frac{\pi}{2}\right)_x - [\tau - (\pi)_y - \tau - \text{echo}]_n, \quad (1c)$$

$$\text{CPMG2} : \left(\frac{\pi}{2}\right)_x - \left[ \begin{array}{l} \tau - (\pi)_y - \tau - \text{echo} \\ \tau - (\pi)_{-y} - \tau - \text{echo} \end{array} \right]_n. \quad (1d)$$

Note that CP1 and CPMG1 are the original CP<sup>35</sup> and CPMG<sup>36</sup> sequences respectively.

We found that by applying the CPMG1 sequence or the CP2 sequence, a magnetization tail appears, i.e. the signal remains for times much longer than  $T_2^{HE}$  as observed in  $^{29}\text{Si}$ .<sup>12</sup> Figure 1 shows the normalized magnetizations acquired by applying the sequences HE; CP1; CP2; CPMG1 and CPMG2 to polycrystalline  $\text{C}_{60}$ . In the last four sequences  $\tau = 1$  ms and signal acquisition is performed at the top of the echo. In all the sequences the durations of the  $\pi$  and  $\pi/2$  pulses were carefully set from nutation experiments to  $7.0 \mu\text{s}$  and  $3.4 \mu\text{s}$ , respectively.

On the other hand, by applying the CP1 or the CPMG2 sequences the decay time is not longer than  $T_2^{HE}$ , but it is remarkable that at short times the magnetization makes a zigzag (consequence of the presence of stimulated echoes) see inset in Fig.1. Besides, the magnetization oscillates going through negative values before reaching its final asymptotic zero value but keeping the  $T_2^{HE}$  decay as envelope (see Fig.2).

By plotting these oscillating decays as a function of the echo number a match of the frequencies can be observed, i.e. the maxima and minima overlap for the same number of  $\pi$  pulses (echo number, see Fig.3). This behavior

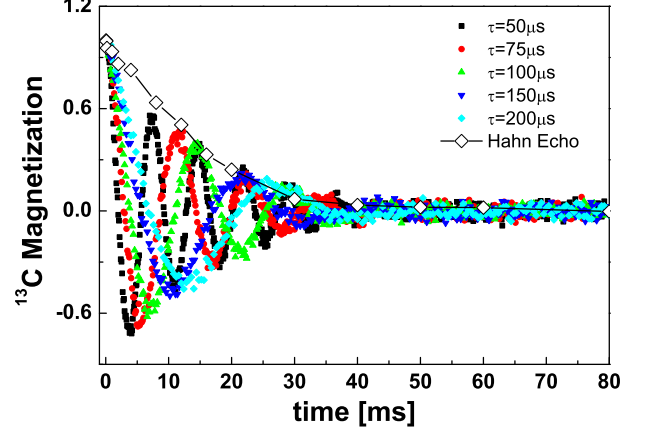


FIG. 2:  $^{13}\text{C}$  Magnetization decay as a function of time measured for different time windows with the CPMG2 sequence in polycrystalline  $\text{C}_{60}$ . It is evident that the envelope of the oscillatory decays are dominated by  $T_{2HE}$ .

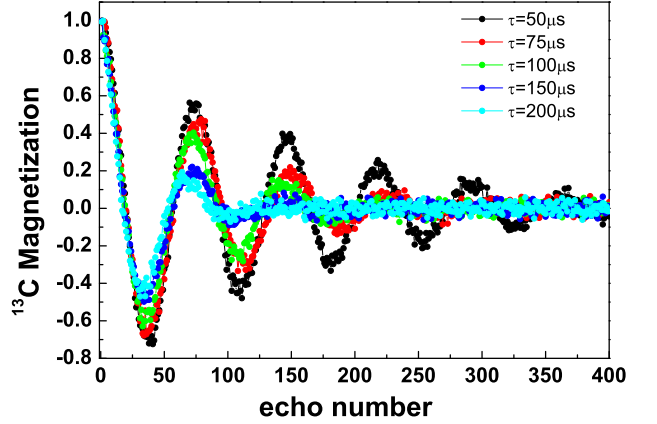


FIG. 3:  $^{13}\text{C}$  Magnetization decays as a function of the number of pulses (or echoes) for short  $\tau$ 's in the CPMG2 sequence.

reveals an accumulation of pulse errors which complete a cycle after approximately 80 pulses. The amplitudes decrease with increasing  $\tau$  following the behavior of the long tails. Note in Fig.1 that for  $\tau = 1$  ms, the oscillation almost disappears.

Another unexpected observation was the presence of noticeable stimulated echoes [STE:  $(\frac{\pi}{2})_x - \tau - (\frac{\pi}{2})_y - t_1 - (\frac{\pi}{2})_y - t$ ] when applying pulse sequences of the form,  $[(\frac{\pi}{2})_x - \tau - (\pi)_{\varphi_2} - t_1 - (\pi)_{\varphi_3} - acq]$  with variable  $\tau$  and  $t_1$ . Indeed, these sequences with  $\pi$  pulses should not produce stimulated echoes. To remember the essentials of the argument we reproduce here our results after the application of the STE sequence with the phases of the CPMG1 and CPMG2, called CPMG1<sup>STE</sup> and CPMG2<sup>STE</sup> respectively in  $\text{C}_{60}$  setting  $\tau = 1$  ms and  $t_1 = 15$  ms (see Fig.4). It can be observed that the stim-

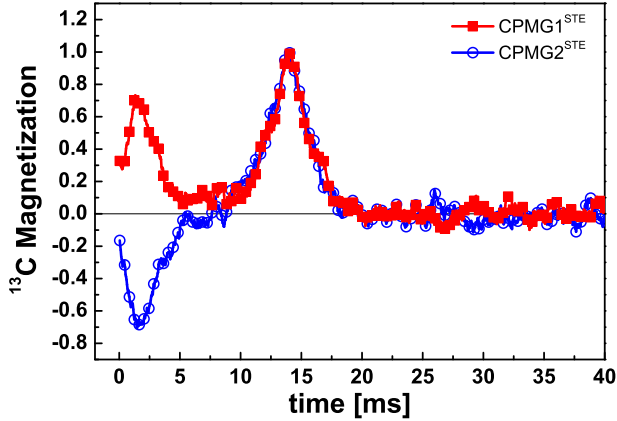


FIG. 4: Stimulated echoes observed with the CPMG1<sup>STE</sup> and CPMG2<sup>STE</sup> sequences in a C<sub>60</sub> polycrystalline sample. The parameters are  $\tau = 1$  ms and  $t_1 = 15$  ms, giving rise to a stimulated and a normal echo at 1 ms and 14 ms after the last pulse, respectively. Notice the inversion of the phase in the stimulated echo.

ulated echoes appear 1 ms after the last pulse (remember that they should not be formed with perfect  $\pi$  pulses) and they show a phase that coincides or it is opposite to that of the Hahn echo, that appears at  $t_1 - \tau = 14$  ms, for the CPMG1<sup>STE</sup> and CPMG2<sup>STE</sup> respectively. A phenomenological explanation for the long magnetization tails based on the constructive or destructive interferences between the stimulated and *normal* echoes was reported by us in a previous paper<sup>43</sup> and later on verified through hole burning experiments<sup>44</sup>. Thus, although disappointing for the experimentalists of the quantum information community, we concluded that the observed long tails in the magnetization decays are not a signature of long decoherence times but of the recovery of coherences saved as polarization. These long pseudocoherent tails appear as a consequence of the formation of stimulated echoes. These echoes, which need at least three pulses to appear, were first observed by E. Hahn<sup>34</sup> and have the particularity that can survive for times as long as the spin-lattice relaxation time  $T_1$ . They will be revised in the next section in order to try to save and recover coherences in a controlled way.

This is the key experiment, and we suggest that this stimulated echo sequence with  $\pi$  pulses,  $[\frac{\pi}{2} - \tau - \pi - 2\tau - \pi - \tau]$  should be used in the same conditions of the CP-like train sequences to be able to discard the stimulated echoes as the origin of the long magnetization tails. Although the presence of the stimulated echoes after this sequence is not expected, they can be generated by the pulse angle distribution present in an inhomogeneously broadened line. In all the samples mentioned above, the spin-spin decay time measured with a Hahn echo sequence ( $T_{2HE}$ )<sup>34</sup> was about an order of magnitude longer than the FID characteristic time ( $T_2^*$ ), evidencing

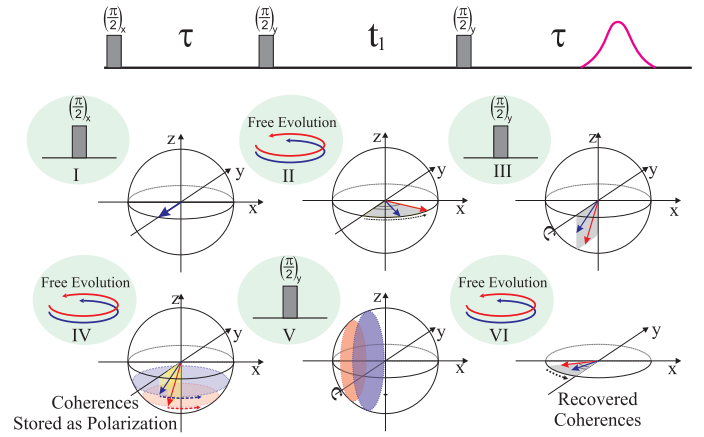


FIG. 5: Traditional stimulated echo sequence. The coherence states created during the first evolution period  $\tau$ , are stored as  $z$ -amplitude (polarization) during  $t_1$  and then reconverted to coherences (transverse magnetization) after the third pulse.

the line inhomogeneity.

Magnetization tails have been observed in <sup>29</sup>Si, C<sub>60</sub> and Y<sub>2</sub>O<sub>3</sub><sup>13,41,42</sup>, in adamantane under <sup>1</sup>H decoupling<sup>57</sup> and indirectly in <sup>31</sup>P in EPR experiments<sup>20</sup>.

The requirements for the formation of the long tails can be summarized as follows: (a) an rf field inhomogeneity or a naturally inhomogeneous line able to produce different tilting angles in different sites of the sample and (b) the absence of or a very slow spin diffusion (noneffective flip-flop interactions). Under these conditions the different tilting angles do not average to the nominal  $\pi$  pulses preset in the sequences leaving a perpendicular component that behaves as in the regular stimulated echo sequence  $[STE : (\frac{\pi}{2})_x - \tau - (\frac{\pi}{2})_y - 2\tau - (\frac{\pi}{2})_y - acq]$  as schematized in Fig.5. Still, one question that remained open was if the relation between the spin-site energy difference and the dipolar couplings (the main source of flip-flop interactions in solid systems) should be verified in a local (microscopic) basis or if a smoothly varying inhomogeneity that only satisfy the relation at longer distances could produce the effect. To investigate this issue we resorted to the use of gradients in homogeneous samples.

We artificially create the necessary conditions to observe the long tails after a CPMG measurement, even for homogeneously broadened samples. The method uses the fact that homogeneous lines, evolving under the influence of a field gradient, are inhomogeneously broadened giving rise to stimulated echoes with the consequent long tails. This method provides a controlled way to move from homogeneous lines (for which the decay observed after a Hahn echo and CPMG like sequences are in complete agreement) to inhomogeneous ones. We reach inhomogeneous limits analogous to <sup>29</sup>Si or C<sub>60</sub> cases, where we show that careful interpretation of the experiments must be done before assigning “the true” spin-spin decay time.

#### IV. BEHAVIOUR OF THE MAGNETIZATION DURING A SIMPLE STIMULATED ECHO SEQUENCE

The stimulated echo contribution to the CPMG sequence has been widely studied in presence of inhomogeneous  $B_0$  and  $B_1$  fields. It has been demonstrated that due to the inaccuracy of the pulses and the off resonance effects, the CPMG echoes have contributions not only from the Hahn echo but also from signals similar to stimulated echoes arising from different coherence pathways<sup>58-60</sup>. This is in complete agreement with our findings.

Here, we review in detail the magnetization evolution during a stimulated echo to make evident how it can be potentially exploited to create memories.

The eigenstates of angular momentum for a spin 1/2 along the static field direction are  $|\uparrow\rangle$  and  $|\downarrow\rangle$ . Once the thermal equilibrium is reached the population of state  $|\uparrow\rangle$  is larger than that of  $|\downarrow\rangle$  indicating a net polarization of spins along the static field direction. This thermal polarization will determine the maximum magnetization that can be created in the system. Any other situation in which the macroscopic magnetization points in an arbitrary direction will eventually have a z-magnetization which reflects a non equilibrium polarization. A particular but very relevant case is the application of a  $\frac{\pi}{2}$  or saturation pulse after which the magnetization lies in the xy plane. The population of the states is equilibrated and converted in a superposition state (a coherence) where the eigenstates  $|\uparrow\rangle$  and  $|\downarrow\rangle$  have the same probability with well defined phase relation. The essential difference between polarization and coherences is that, in a very good approximation, polarization does not evolve under interaction with the static field while the transverse magnetization (or coherence) does.

It is important to correctly understand the processes behind the stimulated echo in order to separate its contribution from the Hahn echo contribution. To clarify the details, let us go back to the simplest stimulated echo sequence:

$$\text{STE} : \left(\frac{\pi}{2}\right)_x - \tau - \left(\frac{\pi}{2}\right)_y - t_1 - \left(\frac{\pi}{2}\right)_y - t \quad (2)$$

In Fig. 5 the stimulated echo formation is schematized using a vectorial spin model. The model provides a pictorial view where it can be observed that the magnetization is indeed stored as polarization and then reconverted to transverse magnetization. The information on the coherence state (characterized by a well defined phase relationship between the transverse spins) created in the first evolution period,  $\tau$ , is conserved during  $t_1$  and refocused as an echo during the third period at  $t = \tau$ .

Let us consider a Hamiltonian linear in the spin operators with no interactions between different spins,

$$\mathcal{H} = \sum_{j=1}^N \delta\omega_j I_j^z. \quad (3)$$

If the delta pulse approximation is taken and we consider the system in thermal equilibrium before the first pulse, the evolution of the density matrix can be written as:

$$\rho(\tau^-) = - \sum_{j=1}^N [\cos(\delta\omega_j \tau) I_j^y - \sin(\delta\omega_j \tau) I_j^x] \quad (4)$$

The expression above represents a coherent state (transverse magnetization), which immediately after the second pulse becomes,

$$\rho(\tau^+) = - \sum_{j=1}^N [\cos(\delta\omega_j \tau) I_j^y + \sin(\delta\omega_j \tau) I_j^z] \quad (5)$$

After the second evolution period ( $t_1$ ), the new state of the system can be expressed as:

$$\rho(\tau + t_1) = - \sum_{j=1}^N \{ \cos(\delta\omega_j \tau) [I_j^y \cos(\delta\omega_j t_1) - I_j^x \sin(\delta\omega_j t_1)] + \sin(\delta\omega_j \tau) I_j^z \} \quad (6)$$

During the time  $t_1$ , there is a component of the initial magnetization stored as non equilibrium polarization in the  $I_j^z$ . This component does not evolve during  $t_1$  under the chemical shift Hamiltonian in Eq. (3). The last term within the sum in Eq.(6) defines a polarization grating which lodges in its amplitude the information of the coherent state, i.e. the phase, of Eq. (4). The useful interpretation is that the coherent state created during the first evolution period remains frozen as a local polarization amplitude during a long period  $t_1$ . It should be noted that during the second period the polarization in Eq. (6) is not in thermal equilibrium (there is not a Boltzmann distribution because of the  $\delta\omega$  dependence). The spin-lattice relaxation, characterized by  $T_1$ , will lead to a decay of the polarization grating during  $t_1$ .

The third  $\left(\frac{\pi}{2}\right)_y$  pulse will convert the polarization of Eq. (6) in transverse magnetization as

$$\rho(\tau + t_1^+) = - \sum_{j=1}^N \{ \cos(\delta\omega_j \tau) [I_j^y \cos(\delta\omega_j t_1) + I_j^z \sin(\delta\omega_j t_1)] + \sin(\delta\omega_j \tau) I_j^x \} \quad (7)$$

which will evolve under the linear Hamiltonian influence

as:

$$\begin{aligned} \rho(t + \tau + t_1) = & - \sum_{j=1}^N \cos(\delta\omega_j\tau) \{ \cos(\delta\omega_j t_1) [I_j^y \cos(\delta\omega_j t) \\ & - I_j^x \sin(\delta\omega_j t)] + I_j^z \sin(\delta\omega_j t_1) \} \\ & + \sin(\delta\omega_j\tau) (I_j^x \cos(\delta\omega_j t) + I_j^y \sin(\delta\omega_j t)) \end{aligned} \quad (8)$$

The last two terms in Eq. (8) do not depend on  $t_1$  and when  $t = \tau$  the phase differences acquired between the spins in the first evolution period are refocused forming the stimulated echo. As can be seen from Eq.(8), if  $t_1=0$  the sequence is reduced to a simple  $(\frac{\pi}{2})_x - \tau - (\pi)_y - \tau -$  Hahn echo sequence and all the initial polarization is again at the -y axis. On the other hand, if  $t_1 \gg T_{2HE}$ , but still shorter than the spin-lattice relaxation time, only the term that do not depend on  $t_1$  survives and the coherences created during the first evolution period are refocused at  $t = \tau$ . Notice that if  $2\tau \approx T_{2HE}$  the dipolar interaction can not be neglected and the assumptions performed in our calculations, where only the chemical shifts were considered, are not valid anymore.

It is straightforward to see that if the second and third pulses in Fig. 5 are  $\pi$  pulses a stimulated echo will not be created<sup>43,61</sup>. Nevertheless if a spatial distribution of flip angles is present in the sample, stimulated echoes will be created due to the deviations from  $\pi$  pulses as shown in ref.<sup>43,60</sup>. The long tails previously observed in inhomogeneous samples are a consequence of a pulse angle distribution among the sample. From Eq.(5) it can be deduced that the long tails observed are due to the formation of stimulated echoes and its consequent storage of local polarization. For example, the magnetization in  $C_{60}$  was stored as polarization for times two orders of magnitude longer than the decoherence time ( $T_{2HE}$ )<sup>41-44</sup>.

## V. CONTROLLED GENERATION OF PSEUDOCOHERENCES

In this section, we introduce a method to artificially create, even in homogeneous samples, the conditions under which the stimulated echoes are formed. The purpose of this method is to study in detail the amplitude of the polarization stored and the time the polarization can be stored as a function of the inhomogeneity added to the sample. Sequences can be developed in order to take advantage of this stored polarization<sup>20</sup>.

The system we have previously studied,  $C_{60}$ , presents an inhomogeneously broadened line which satisfies  $T_{2HE} \approx 7T_2^*$ . Similar situations were observed in all the systems that manifest long decay times when CPMG-like sequences are applied<sup>12,43,44</sup>.

Here, we use a homogeneous sample to mimic the behaviour observed in inhomogeneous samples by adding magnetic field gradients. When a field gradient,  $G = \partial B_z / \partial z$ , is applied in the direction of the static magnetic field  $B_0 \mathbf{z}$ , the z component of the magnetic field is written as:

$$B_z = B_0 + zG. \quad (9)$$

As a consequence of the field gradient presence, the spin frequency is modified as follows:

$$\omega(z) = \omega_0 + \omega_G(z) \quad (10)$$

where  $\omega_G(z) = \gamma Gz$ , with  $\gamma$  the gyromagnetic factor.

Similarly to Eq.(3), the field gradient produces a Hamiltonian linear in spin operators. If a strong enough gradient is applied, the main interaction for the spin evolution is:

$$\mathcal{H}_G = \gamma \hbar G \sum I_i^z z_i. \quad (11)$$

The presence of this Hamiltonian term causes an inhomogeneously broadened line whose width depends on the applied field gradient.

In the present work the sample used as example is polydimethylsiloxane (PDMS)<sup>62,63</sup>. The characteristic time decays for the PDMS are  $T_2^* \approx 0.6$  ms and  $T_{2HE} \approx 1.8$  ms indicating a small inhomogeneity in the system. The condition  $T_{2HE} \approx 7 T_2^*$  found in  $C_{60}$  is easily satisfied with a field gradient of strength around 5 G/cm. All the experiments were performed at 7 Tesla in a Bruker AvanceII. A birdcage coil of 10 mm ID and Bruker microimaging coils were used. The pulse durations were 12.5  $\mu$ s for the  $\frac{\pi}{2}$  and 25.5  $\mu$ s for the  $\pi$  pulses.

To validate the proposed method we applied a  $(\frac{\pi}{2})_x - \tau - (\pi)_y - t_1 - (\pi)_y$  sequence with  $\tau = 0, 5$  ms and  $t_1 = 8$  ms with and without field gradient, see Fig.6. The temporal windows are chosen such that the refocalization of Hahn and stimulated echoes are produced at different times, remember that for perfect  $\pi$  pulses no stimulated echoes are expected. However, even in absence of the external field gradient a small stimulated echo is observed due to the sample inhomogeneity mentioned before. Notice that its amplitude is approximately eight times smaller than the Hahn echo amplitude after approximately  $4 \times T_{2HE}$ . Upon application of the external field gradient  $G$ , the Hahn echo signal is spread into different frequency components keeping the amplitude constant, while the stimulated echo increases depending on  $G$ . It is clear that under the interpulse timings required by the CPMG ( $t_1=2\tau$ ) the STE overlaps the Hahn echo. By applying proper phase cycling schemes, the discrimination of these two echoes becomes possible<sup>44</sup>.

In Fig. 7 the STE is normalized with the amplitude of the HE to give its relative contribution as a function of the applied gradient field  $G$ . Two datasets were acquired with the proper phase cyclings in order to obtain the stimulated and the Hahn echoes independently. It is noticeable that the stimulated echo grows quadratically with the magnitude of the applied field gradient.

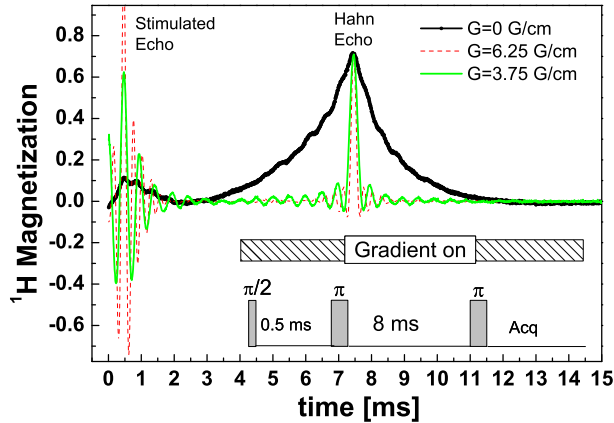


FIG. 6: Stimulated echo formation in presence of field gradients for the three-pulse sequence shown at the bottom of the figure. Notice that while the Hahn echo amplitude remains constant the stimulated echo increases with the magnitude of the applied field gradient.

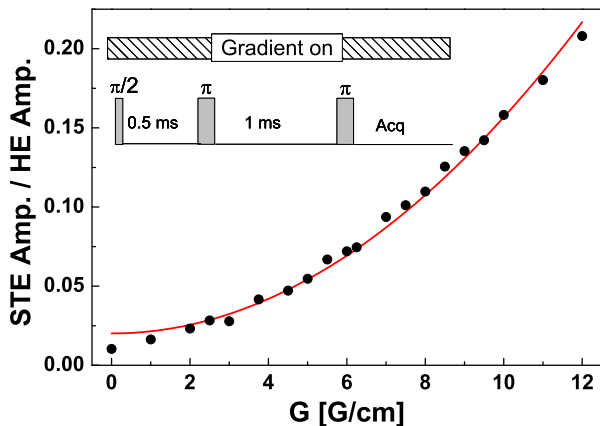


FIG. 7: Stimulated echo amplitude normalized with the corresponding Hahn echo amplitude as a function of the applied field gradient. By fitting the data with the function  $aG^2 + b$  the parameters  $a = 0.00137 \left(\frac{\text{G}}{\text{cm}}\right)^{-2}$  and  $b = 0.02$  are obtained, straight line in the plot.

## VI. LONG TAILS GENERATED USING MAGNETIC FIELD GRADIENTS

As reviewed in Section III, and Figs.1-4, we analyzed<sup>43</sup>, two different sequences derived from Carr–Purcell<sup>35</sup> and Carr–Purcell–Meiboom–Gill<sup>36</sup> which produce long decay times compared to the Hahn echo in inhomogeneous samples, namely CP2 and CPMG1 (see Fig.1). In this section, the evolution of the magnetization during these sequences is studied upon variations of external field gradients and interpulse spacing. In absence of an external field gradient the decays observed with the multipulse

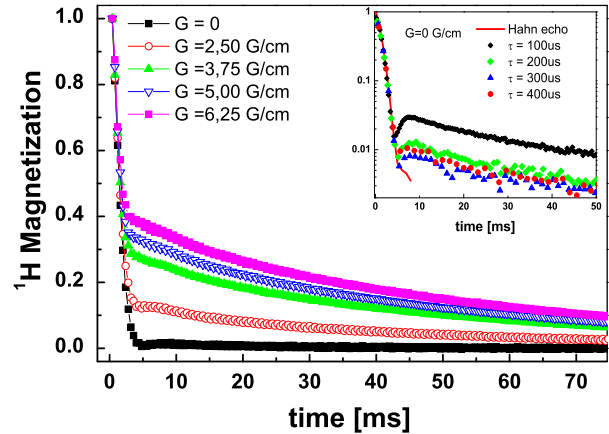


FIG. 8: Magnetization as a function of time for  $\tau = 200 \mu\text{s}$  and several field gradient strengths in the CP2 sequence. The Hahn echo and CP2 decays are very similar in the absence of field gradients. The inset shows the evolution of the magnetization for different values of  $\tau$  when  $G = 0$ . Notice the change of the trend in the amplitudes between  $\tau = 300$  and  $\tau = 400 \mu\text{s}$

CPMG1 and CP2 and the Hahn echo sequences in PDMS are almost the same. There is however a low contribution (c.a. 3%) with decay time of 40 ms that can be observed by using a logarithmic scale in the inset of Fig. 8. This is a consequence of the very small contribution of the stimulated echo generated by the small inhomogeneity of the line even when  $G = 0$ . Notice that the amplitudes of the tails decrease from  $\tau = 100 \mu\text{s}$  to  $\tau = 300 \mu\text{s}$ , while at  $\tau = 400 \mu\text{s}$  this trend reverses.

In Fig. 8 we show the dependence of the magnetization as a function of time for different field gradients for the CP2 sequence at a fixed value  $\tau = 200 \mu\text{s}$ . As stronger field gradients are applied during the complete pulse train for both CP2 and CPMG1, bigger amplitudes of the slow decaying contributions appear manifesting the storage of coherences.

As observed in C60, the magnetization decay in PDMS under gradients manifests two different contributions. For short times, the Hahn echo is dominant while for long times only the stimulated echo remains, storing polarization which is then recovered as transverse magnetization. In order to characterize the decays the data were fitted with a double exponential, where the short characteristic time was fixed to the  $T_{2HE}$  decay time.

$$M(2\tau) = A_s \exp(2\tau/T_{2HE}) + A_l \exp(2\tau/t_l)$$

The parameters  $A_s$ ,  $A_l$  and  $t_l$ , where the subindexes  $s$  and  $l$  stand for short and long decays respectively, were calculated by fitting each dataset individually. The parameters  $A_l$  and  $t_l$  are signatures of the stimulated echoes manifested through the long tails. A more detailed analysis of the long tails was achieved by discarding the short time points and fitting to a single exponential. In Figs. 9

and 10 the percentage of magnetization stored as polarization ( $A_l/A_s \times 100$ ) and the corresponding values for the inverse of the characteristic long decay times  $t_l$  respectively are shown as a function of the inter-pulse time scaled by  $T_{2HE}$  in the CPMG2 sequence. From Fig.9, it can be seen that for the strongest gradient applied and for the shortest  $\tau$ , more than 35% of the initial magnetization was stored as polarization and then refocused during the multipulse sequence. The characteristic decay time  $t_l$  of the long tails, is interpreted as a storage time and the scaling with  $T_{2HE}$  emphasizes the fact that the magnetization can be preserved for times an order of magnitude longer than the single-spin decoherence time. Under favorable experimental conditions  $2\tau/T_{2HE}$  can be decreased to get a better  $t_l/T_{2HE}$  ratio. This amount can also be improved when shorter delays  $\tau$  are experimentally affordable.

A remarkable behaviour of  $1/t_l$  vs.  $\tau$  is plotted Fig.10 for different values of the gradient  $G$ . A change of regime occurs at approximately  $\tau_c = 450 \mu s$  corresponding to  $t_l \approx 40$  ms, the same relaxation time that is obtained in the absence of gradients. For values of  $\tau$  shorter than  $\tau_c$ , the linewidth  $\Delta\nu$  decreases (i.e. the characteristic long time  $t_l$  increases) as the magnitude of the gradient increases (see Fig. 11). For times longer than  $\tau_c$ , the behavior reverses, i.e.  $t_l$  decreases as  $G$  increases. This is more clearly appreciated in Fig.11 where the values of  $t_l$  for different values of  $\tau$  are plotted vs. the magnitude of the gradient  $G$ . It is seen that for  $\tau \leq 400 \mu s$   $t_l$  increases with the gradient while for  $\tau \geq 500 \mu s$   $t_l$  decreases with  $G$ . This  $\tau_c$  (interpulse time  $900 \mu s$ ) should be related to the characteristic fluctuation time of the bath  $\tau_b$ , or its spectral density, essentially dominated by dipolar interactions partially averaged by motion. In a simple picture, one can interpret that a fast interpulse rate ( $1/(2\tau_c) \gg 1/\tau_b$ ) produces a decoupling of the system from the bath, leading to narrower lines (longer  $t_l$  values) while the opposite condition leads to a broadening of the line. In other terms, one can assume that at short values of  $\tau$  ( $\tau \ll 1/d$ ) where  $d$  stands for the magnitude of the dipolar interaction, there is an "effective dipolar interaction" given by  $d_{eff} = d^2\tau$  as the pulses act as a breaking time or  $1/\tau$  as an exchange rate in an exchange narrowing process<sup>64</sup>. In this regime, dipolar spin dynamics are very slow. When  $\tau \geq 1/d$ , the spin diffusion, which is able to average the deviation of the  $\pi$  pulses which lead to the formation of stimulated echoes, is also effective to blur out the gradients in the sample. Then, even with larger gradients, the values of  $t_l$  decrease spoiling the preservation of coherences as polarization. While a deeper analysis of how the dynamical variables  $d$ ,  $\tau$ , and  $\gamma G$  interact is beyond the scope of this article, one conclusion is clear: in order to save coherences as polarization the shortest  $\tau$  and the biggest  $G$  should be used. This can even allow a manipulation of nuclear spins with better spatial resolution. As it is clear from Eq.(8), and schematized in Fig.5, the STE sequence is not able to recover the whole coherence, but

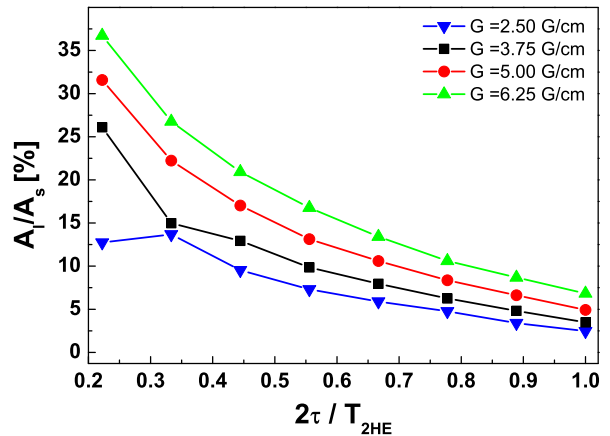


FIG. 9: Percentage of magnetization stored as polarization as function of the inter-pulse time  $2\tau$  scaled by  $T_{2HE}$  in the multipulse sequence CP2. Better performance is achieved by increasing the field gradients and/or decreasing  $\tau$ .

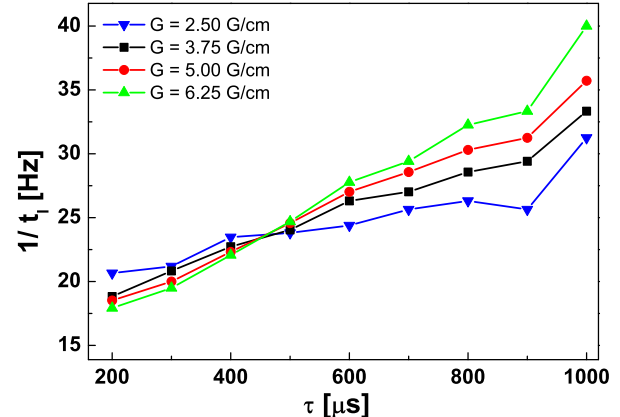


FIG. 10: Characteristic linewidth  $1/t_l$  as function of  $\tau$  in the multipulse sequence CP2. Note the crossing point at approximately  $450 \mu s$

at most 1/2 of its initial amplitude. Consequently, this strategy is not useful to make "quantum memories" (fidelity below 0.66). Nevertheless, it is potentially useful to make read out memories. Moreover, in a different context, Kobayashi et al.<sup>65</sup> have designed variations of the STE sequence that overcome the 1/2 factor and recover a much bigger fraction of the coherences (or transverse magnetization).

Finally, we address the possibility of performing experiments with multipulse sequences that do not produce coherence storage as polarization. A four phase cycle



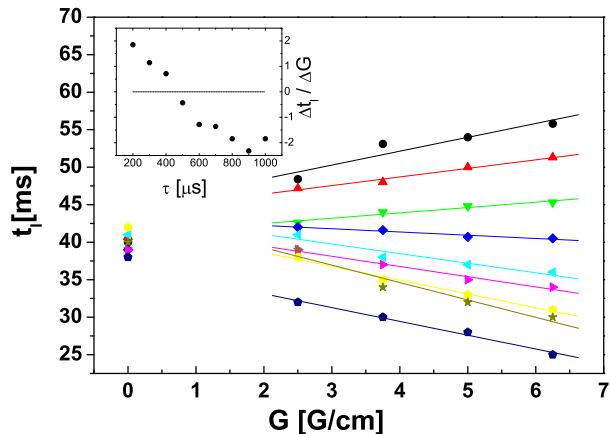


FIG. 11: Characteristic long decay rate as a function of the field gradient. Different values of  $\tau$ , which scale the dipolar dynamics ( $d_{\text{eff}} \simeq d^2\tau$ ), from top to bottom, 200, 300, 400, 500, 600, 700, 800, 900 and 1000  $\mu\text{s}$  are displayed. Note the change of slope between 400 and 500  $\mu\text{s}$ . This is emphasized in the inset where the slopes are plotted as a function of  $\tau$ . The change of sign identifies the critical value. The decay of  $t_l = 40\text{ms}$  for  $G = 0$  is due to line inhomogeneities and shimming imperfections

sequence that resembles the MLEV-4<sup>45</sup>:

$$\text{CPMG4} : \left( \frac{\pi}{2} \right)_x \left( \begin{array}{l} - (\tau - \pi_y - \tau - \text{echo} \\ - \tau - \pi_y - \tau - \text{echo} \\ - \tau - \pi_{-y} - \tau - \text{echo} \\ - \tau - \pi_{-y} - \tau - \text{echo} \end{array} \right)_n \quad (12)$$

has been empirically shown to be the most suitable for preventing unexpected artifacts in a  $T_2$  measurement<sup>46,47</sup>.

In Fig. 12 the results of a Hahn echo and CPMG4 measurements with and without field gradient are plotted. It can be observed that the magnetization decay agrees perfectly well for the three cases. The reason why this sequence is the appropriate to measure  $T_2$  can be understood from the stimulated echo perspective presented previously<sup>43</sup>. The CPMG4 sequence does not accumulate magnetization contributions from the constructive interference between normal and stimulated echoes, and this is clearly manifested in the results shown in Fig. 12. Even in the presence of an inhomogeneous field, long tails are not observed when this sequence is applied.

## VII. CONCLUSIONS

In this article, we have reviewed the conditions for the formation of stimulated echoes and the consequent generation of long tails in the magnetization decay. Besides, we report an original set of experiments using field gradients in homogeneous samples that extend and validates

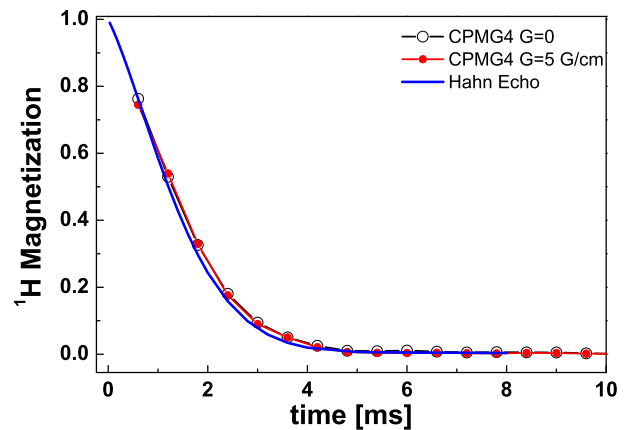


FIG. 12: Magnetization observed by applying the CPMG4 with gradient off and on compared to the Hahn Echo decay.

the previous findings and their interpretation. Moreover, they suggest a controlled way to preserve coherences as polarization that may account for more than 1/3 of the original signal. The long tails observed when multipulse sequences as CPMG are applied to inhomogeneous samples were assigned to polarization that encodes quantum coherences. In this way the coherences are stored for times much longer than  $T_{2\text{HE}}$ . It has been shown that the responsible of the long tails are the stimulated echoes, formed due to the inhomogeneity of the sample. The requirements to observe these slow magnetization decays are (1) an rf field inhomogeneity or a highly inhomogeneous line able to produce different tilting angles in different sites of the sample and (2) non-effective flip-flop interactions. Under these conditions the differences in resonance frequencies are larger than the dipolar couplings, making ineffective the flip-flop mechanism. Consequently, the different deviations from  $\pi$  pulses (regardless of its origin) cannot be averaged out by dipolar interactions. For  $2\tau \approx T_{2\text{HE}}$  the amplitude of the coherence stored is less than 5%. In this condition, the time between pulses is enough for the dipolar interaction to be operative.

In this paper we showed that the stimulated echoes preserve coherent states frozen in the direction of the static magnetic field, then bring them back to the plane where they are refocused and observed. It is important to remark that the magnetization decay is very long because the coherences are stored as polarization. So, these long decays should not be interpreted as a long decoherence time during which quantum operations can be performed. However, this strategy can be exploited to design memories in nuclear or electron spin systems. Then, upon recovery of the stored coherences, interactions among the whole system can be turned on. The concept introduced in this paper was indeed indirectly exploited in Ref.<sup>20</sup>. There, coherences induced in electron spins were transferred to a coherent state between nuclear spins, stored

by applying the CPMG1 sequence and transferred back to electron spins.

The method that mimic the conditions to induce the stimulated echoes for homogeneous samples in a controlled way is based on the application of field gradients that produce a frequency distribution across the sample. This, in turn, generates a pulse angle distribution that sets the conditions under which the stimulated echoes appear. An important fact deduced from these experiments is that the origin of the inhomogeneity of the samples is not relevant for the observation of long tails. Whether the inhomogeneity arises from a random distribution of nuclear spins (as occurs in  $^{29}\text{Si}$ ) or on a linear dependent gradient, like the one used in the present experiments, the consequences are the same. Moreover, the use of suitable field gradients could allow a more selective spatial manipulation of the memories. This method was applied to a PDMS sample, for which we were able to perform a complete quantification of the procedure, i.e. the storage time and ratio of coherence survival. There, it was possible to detect a transition where the effective dipolar interaction  $d^2\tau$  becomes of the order of the main frequencies in the bath's spectral density. This imposes a limit in

the interpulse spacing in which coherences can be stored. Under the condition  $\tau < 1/d$  higher polarization storage and longer decay times are achieved by using stronger gradients.

Finally, we tested the CPMG4 sequence under field gradients that reproduce inhomogeneous properties. The mechanism behind the correct operation of this pulse sequence can be understood under the stimulated echoes interferences. The true single-spin  $T_2$  decay time can be measured under this pulse sequence either for homogeneous or inhomogeneous samples. Thus, we verified the empirically known robustness of this sequence which, regardless of the gradient, yields the same results as the Hahn echo.

We acknowledge support from Fundación Antorchas, CONICET, FoNCyT, MinCyT-Cor SeCyT-UNC and the Partner Group for NMR Spectroscopy with High Spin Polarization FaMAF-MPIP. We thank M. A. Villar, E. M. Vallés and D. A. Vega for sample preparation, A. D. Dente for helping in the design of Fig. 5, G. A. Monti and F.M. Pastawski for helpful discussions.

\* Electronic address: franzoni@mpip-mainz.mpg.de

† Electronic address: racosta@famaf.unc.edu.ar

‡ Electronic address: horacio@famaf.unc.edu.ar

§ Electronic address: patricia@famaf.unc.edu.ar

<sup>1</sup> D. P. DiVincenzo. Quantum computation. *Science*, 270:255–261, 1995.

<sup>2</sup> D. G. Cory, A. F. Fahmy, and T. F. Havel. Ensemble quantum computing by nmr spectroscopy. *Proc. Natl. Acad. Sci. U.S.A.*, 94:1634, 1997.

<sup>3</sup> C. H. Bennett and D. P. Divincenzo. Quantum information and computation. *Nature*, 404(6775):247–255, 2000.

<sup>4</sup> W. H. Zurek. Decoherence, eigenselection, and the quantum origins of the classical. *Reviews of Modern Physics*, 75:715, 2003.

<sup>5</sup> W. H. Zurek, F. M. Cucchiatti, and J. P. Paz. Gaussian decoherence and gaussian echo from spin environments. *Acta Physica Polonica Series B*, 38(5):1685, 2006.

<sup>6</sup> G. A. Álvarez, E. P. Danieli, P. R. Levstein, and H. M. Pastawski. Environmentally induced quantum dynamical phase transition in the spin swapping operation. *The Journal of Chemical Physics*, 124(19):194507, 2006.

<sup>7</sup> Wenxian Zhang, N. Konstantinidis, K. A. Al-Hassanieh, and V. V. Dobrovitski. Modelling decoherence in quantum spin systems. *J. Phys. Cond. Matt.*, 19:083202, 2007.

<sup>8</sup> G. A. Álvarez, E. P. Danieli, P. R. Levstein, and H. M. Pastawski. Decoherence under many-body system-environment interactions: A stroboscopic representation based on a fictitiously homogenized interaction rate. *Physical Review A*, 75(6):062116, June 2007.

<sup>9</sup> C. M. Sánchez, P. R. Levstein, R. H. Acosta, and A. K. Chattah. NMR loschmidt echoes as quantifiers of decoherence in interacting spin systems. *Phys. Rev. A*, 80:012328, 2009.

<sup>10</sup> H. G. Krojanski and D. Suter. Scaling of decoherence in

wide NMR quantum registers. *Phys. Rev. Lett.*, 93:090501, 2004.

<sup>11</sup> H. G. Krojanski and D. Suter. Reduced decoherence in large quantum registers. *Phys. Rev. Lett.*, 97:150503, 2006.

<sup>12</sup> A. E. Dementyev, D. Li, K. MacLean, and S. E. Barrett. Anomalies in the nmr of silicon: unexpected spin echoes in a dilute dipolar solid. *Phys. Rev. B*, 68:153302, 2003.

<sup>13</sup> T. D. Ladd, D. Maryenko, Y. Yamamoto, E. Abe, and K. M. Itoh. Coherence time of decoupled nuclear spins in silicon. *Phys. Rev. B*, 71:014401, 2005.

<sup>14</sup> P. Cappellaro, C. Ramanathan, and D. G. Cory. Simulations of information transport in spin chains. *Phys. Rev. Lett.*, 99:250506, Dec 2007.

<sup>15</sup> P. Cappellaro, C. Ramanathan, and D. G. Cory. Dynamics and control of a quasi-one-dimensional spin system. *Phys. Rev. A*, 76:032317, Sep 2007.

<sup>16</sup> E. Rufeil-Fiori, C. M. Sánchez, F. Y. Oliva, H. M. Pastawski, and P. R. Levstein. Effective one-body dynamics in multiple-quantum NMR experiments. *Phys. Rev. A*, 79:032324, 2009.

<sup>17</sup> P. R. Levstein, G. Usaj, and H. M. Pastawski. Attenuation of polarization echoes in nuclear magnetic resonance: A study of the emergence of dynamical irreversibility in many-body quantum systems. *J. Chem. Phys.*, 108:2718–2724, 1998.

<sup>18</sup> G. A. Álvarez and D. Suter. NMR quantum simulation of localization effects induced by decoherence. *Physical Review Letters*, 104(23):230403, June 2010.

<sup>19</sup> M. Mehring, W. Scherer, and A. Weidinger. Pseudoentanglement of spin states in the multilevel N15@C60 system. *Phys. Rev. Lett.*, 93, 2004.

<sup>20</sup> J. J. L. Morton, A. M. Tyryshkin, R. M. Brown, S. Shankar, B. W. Lovett, A. Ardavan, T. Schenkel, E. E. Haller, J. W. Ager, and S. A. Lyon. Solid-state quantum

- memory using the 31P nuclear spin. *Nature*, 455:1085–1088, 2008.
- 21 L. Childress, M. V. Gurudev Dutt, J. M. Taylor, A. S. Zibrov, F. Jelezko, J. Wrachtrup, P. R. Hemmer, and M. D. Lukin. Coherent dynamics of coupled electron and nuclear spin qubits in diamond. *Science*, 314(5797):281–285, 2006.
  - 22 Nan Zhao, Zhen-Yu Wang, and Ren-Bao Liu. Anomalous decoherence effect in a quantum bath. *Physical Review Letters*, 106(21):217205, May 2011.
  - 23 G. D. Fuchs, G. Burkard, P. V. Klimov, and D. D. Awschalom. A quantum memory intrinsic to single nitrogen-vacancy centres in diamond. *Nat Phys*, 7(10):789–793, October 2011.
  - 24 J. Baugh, O. Moussa, C. A. Ryan, R. Laflamme, C. Ramanathan, T. F. Havel, and D. G. Cory. Qubit coherence control in a nuclear spin bath. *Phys. Rev. A*, 73:022305, 2006.
  - 25 G. de Lange, Z. H. Wang, D. Riste, V. V. Dobrovitski, and R. Hanson. Universal dynamical decoupling of a single Solid-State spin from a spin bath. *Science*, 330(6000):60–63, October 2010.
  - 26 H. Bluhm, S. Foletti, I. Neder, M. Rudner, D. Mahalu, V. Umansky, and A. Yacoby. Dephasing time of GaAs electron-spin qubits coupled to a nuclear bath exceeding 200  $\mu$ s. *Nature Physics*, 7(2):109–113, February 2011.
  - 27 C. A. Ryan, J. S. Hodges, and D. G. Cory. Robust decoupling techniques to extend quantum coherence in diamond. *Physical Review Letters*, 105(20):200402, November 2010.
  - 28 C. Barthel, J. Medford, C. M. Marcus, M. P. Hanson, and A. C. Gossard. Interlaced dynamical decoupling and coherent operation of a Singlet-Triplet qubit. *Physical Review Letters*, 105(26):266808, December 2010.
  - 29 J. R. Petta, A. C. Johnson, J. M. Taylor, E. A. Laird, A. Yacoby, M. D. Lukin, C. M. Marcus, M. P. Hanson, and A. C. Gossard. Coherent manipulation of coupled electron spins in semiconductor quantum dots. *Science*, 309(5744):2180–2184, 2005.
  - 30 J. M. Martinis, S. Nam, J. Aumentado, and C. Urbina. Rabi oscillations in a large josephson-junction qubit. *Phys. Rev. Lett.*, 89:117901, Aug 2002.
  - 31 D. Vion, A. Aassime, A. Cottet, P. Joyez, H. Pothier, C. Urbina, D. Esteve, and M. H. Devoret. Manipulating the quantum state of an electrical circuit. *Science*, 296(5569):886–889, 2002.
  - 32 R. Hanson, L. P. Kouwenhoven, J. R. Petta, S. Tarucha, and L. M. K. Vandersypen. Spins in few-electron quantum dots. *Reviews of Modern Physics*, 79(4):1217, 2007.
  - 33 M. J. Biercuk, H. Uys, A. P. VanDevender, N. Shiga, W. M. Itano, and J. J. Bollinger. Optimized dynamical decoupling in a model quantum memory. *Nature*, 458(7241):996–1000, 2009.
  - 34 E. L. Hahn. Spin echoes. *Phys. Rev.*, 80:580, 1950.
  - 35 H. Y. Carr and E. M. Purcell. Effects of diffusion on free precession in nuclear magnetic resonance experiments. *Phys. Rev.*, 94:630, 1954.
  - 36 S. Meiboom and D. Gill. Modified Spin-Echo method for measuring nuclear relaxation times. *Rev. Sci. Instrum.*, 29:688–691, 1958.
  - 37 L. Viola, E. Knill, and S. Lloyd. Dynamical decoupling of open quantum systems. *Physical Review Letters*, 82(12):2417–2421, March 1999.
  - 38 G. S. Uhrig. Keeping a quantum bit alive by optimized  $\pi$ -Pulse sequences. *Physical Review Letters*, 98(10):100504, March 2007.
  - 39 G. A. Álvarez, A. Ajoy, X. Peng, and D. Suter. Performance comparison of dynamical decoupling sequences for a qubit in a rapidly fluctuating spin bath. *Phys. Rev. A*, 82:042306, Oct 2010.
  - 40 Wen Yang, Zhen-Yu Wang, and Ren-Bao Liu. Preserving qubit coherence by dynamical decoupling. *Frontiers of Physics*, 6:2–14, September 2010.
  - 41 Dale Li, A. E. Dementyev, Y. Dong, R. G. Ramos, and S. E. Barrett. Generating unexpected spin echoes in dipolar solids with  $\pi$  pulses. *Phys. Rev. Lett.*, 98:190401, May 2007.
  - 42 D. Li, Y. Dong, R. G. Ramos, J. D. Murray, K. MacLean, A. E. Dementyev, and S. E. Barrett. Intrinsic origin of spin echoes in dipolar solids generated by strong  $\pi$  pulses. *Phys. Rev. B*, 77:214306, Jun 2008.
  - 43 M. B. Franzoni and P. R. Levstein. Manifestations of the absence of spin diffusion in multipulse NMR experiments on diluted dipolar solids. *Phys. Rev. B*, 72:235410, 2005.
  - 44 M. B. Franzoni, P. R. Levstein, J. Raya, and J. Hirschinger. Hole burning in polycrystalline c60: An answer to the long pseudocoherent tails. *Phys. Rev. B*, 78:115407, 2008.
  - 45 T. Frenkiel M. H. Levitt, R. Freeman. *Advances in Magnetic Resonance*, volume 11. Academic Pr, 1983.
  - 46 Terry Gullion, David B. Baker, and Mark S. Conradi. New, compensated Carr-Purcell sequences. *Journal of Magnetic Resonance (1969)*, 89(3):479–484, 1990.
  - 47 K. Saalwächter, B. Herrero, and M. A. López-Manchado. Chemical Shift-Related artifacts in NMR determinations of proton residual dipolar couplings in elastomers. *Macrom.*, 38:4040–4042, 2005.
  - 48 S. Zhang, B. H. Meier, and R. R. Ernst. Polarization echoes in nmr. *Phys. Rev. Lett.*, 69:2149–2151, Oct 1992.
  - 49 W-K. Rhim, D. D. Elleman, and R. W. Vaughan. Analysis of multiple pulse NMR in solids. *J. Chem. Phys.*, 59:3740–3749, 1973.
  - 50 D. G. Cory, J. B. Miller, and A. N. Garroway. Time suspension multiple-pulse sequences; applications to solid-state imaging. *J. Magn. Res.*, 90:205–213, 1990.
  - 51 H. M. Pastawski, P. R. Levstein, G. Usaj, J. Raya, and J. Hirschinger. A nuclear magnetic resonance answer to the boltzmann-loschmidt controversy? *Phys. A*, 283:166, 2000.
  - 52 R. A. Jalabert and H. M. Pastawski. Environment-independent decoherence rate in classically chaotic systems. *Phys. Rev. Lett.*, 86:2490–2493, Mar 2001.
  - 53 T. Gorin, T. Prosen, T. H. Seligman, and M. Znidaric. Dynamics of loschmidt echoes and fidelity decay. *Phys. Rep.*, 435:33, 2006.
  - 54 Ph. Jacquod and C. Petitjean. Decoherence, entanglement and irreversibility in quantum dynamical systems with few degrees of freedom. *Advances in Physics*, 58(2):67–196, 2009.
  - 55 B.E. Kane. A silicon-based nuclear spin quantum computer. *Nature*, 393:133, 1998.
  - 56 S. Watanabe and S. Sasaki. 29si nuclear-spin decoherence process directly observed by multiple spin-echoes for pure and carrier-less silicon. *Jpn. J. Appl. Phys.*, 42:L1350, 2003.
  - 57 A. M. Souza, G. A. Álvarez, and D. Suter. Robust dynamical decoupling for quantum computing and quantum memory. *Phys. Rev. Lett.*, 106:240501, Jun 2011.
  - 58 M. D. Hurlimann and D. D. Griffin. Spin dynamics of Carr Purcell Meiboom Gill like sequences in grossly inhomogeneous B0 and B1 fields and application to NMR well

- logging. *J. Magn. Reson.*, 143:120–135, 2000.
- <sup>59</sup> M. Hurlimann. Diffusion and relaxation effects in general stray field NMR experiments. *J. Magn. Reson.*, 148:367–378, 2001.
- <sup>60</sup> Y.-Q. Song. Categories of coherence pathways for the CPMG sequence. *J. Magn. Reson.*, 157:82–91, 2002.
- <sup>61</sup> M. Mehring and V. A. Weberruß. *Object-Oriented Magnetic Resonance*. Academic Press, 2001.
- <sup>62</sup> R. H. Acosta, G. A. Monti, M. A. Villar, E. M. Valles, and D. A. Vega. Transiently trapped entanglements in model polymer networks. *Macrom.*, 42:4674–4680, 2009.
- <sup>63</sup> R. H. Acosta and G. A. Monti. Private Communication. *A double quantum filter before each pulse sequence was applied to select the contribution of the elastic chains, i.e. the solid like behavior.*
- <sup>64</sup> P. W. Anderson. A mathematical model for the narrowing of spectral lines by exchange or motion. *J. Phys. Soc. Jpn.*, 9:316–339, 1954.
- <sup>65</sup> T. Kobayashi, J. A. DiVerdi, R. A. Faulkner, and G. E. Maciel. Saving transverse magnetization. *Solid State Nuclear Magnetic Resonance*, 36(4):202 – 208, 2009.